The EMBO Journal vol.13 no.12 pp.2849–2861, 1994

A thermodynamic scale for leucine zipper stability and dimerization specificity: e and g interhelical interactions

Dmitry Krylov, Irina Mikhailenko and Charles Vinson

Building 37, Room 4D06, Laboratory of Biochemistry, National Cancer Institute, National Institutes of Health, Bethesda, MD 20892, USA

Communicated by U.Schibler

The leucine zipper is a dimeric coiled-coil protein structure composed of two amphipathic α-helices with the hydrophobic surfaces interacting to create the dimer interface. This structure has been found to mediate the dimerization of two abundant classes of DNA binding proteins: the bZIP and bHLH-Zip proteins. Several workers have reported that amino acids in the e and g positions of the coiled coil can modulate dimerization stability and specificity. Using the bZIP protein VBP as a host molecule, we report a thermodynamic scale ($\Delta\Delta G$) for 27 interhelical interactions in 35 proteins between amino acids in the g and the following e positions (g⟷e′) of a leucine zipper coiled coil. We have examined the four commonly occurring amino acids in the e and g positions of bZIP proteins, lysine (K), arginine (R), glutamine (Q), glutamic acid (E), as well as the only other remaining charged amino acid aspartic acid (D), and finally alanine (A) as a reference amino acid. These results indicate that E⟷R is the most stable interhelical pair, being 0.35 kcal/mol more stable than E⟷K. A thermodynamic cycle analysis shows that the E⟷R pair is 1.33 kcal/mol more stable than A⟷A with −1.14 kcal/mol of coupling energy ($\Delta\Delta G_{int}$) coming from the interaction of E with R. The E⟷K coupling energy is only −0.14 kcal/mol. E interacts with more specificity than Q. The R⟷R pair is less stable than the K⟷K by 0.24 kcal/mol. R interacts with more specificity than K. Q forms more stable pairs with the basic amino acids K and R rather than with E. Changing amino acids in the e position to A creates bZIP proteins that form tetramers.

Key words: coiled coil/dimerization specificity/leucine zipper/thermodynamic cycle

Introduction

The coiled coil is a helical protein motif that forms a variety of oligomers: dimers, trimers and tetramers (Cohen and Parry, 1990; O'Shea *et al.*, 1991; Alberti *et al.*, 1993; Harbury *et al.*, 1993; Lovejoy *et al.*, 1993). Dimeric coiled coils have a seven-residue repeat of hydrophobic and hydrophilic amino acids capable of forming an amphipathic α-helix (Figure 1A). In order to generate a repeating helical dimerization interface, the α-helix over-twists slightly, going from 3.6 to 3.5 amino acids/turn. This results in a repeating structural unit of two helical turns or seven amino acids (a heptad repeat). The **a** and **d** residues are hydrophobic and pack in a regular 'knobs and holes' pattern (Crick, 1953) along the dimerization interface. This creates the hydrophobic core that stabilizes the coiled coil and is critical for dimerization. The **e** and **g** positions which flank the dimerization interface contain a large number of charged amino acids and have been thought to interact electrostatically (Figure 1A) (Cohen and Parry, 1990; Alber, 1992; Baxevanis and Vinson, 1993). Recent work from Kim and Alber's groups (Harbury *et al.*, 1993) has shown that leucine in the **d** position is a critical determinant of the oligomerization properties of coiled coils; leucine favors dimers. This result suggests that the term leucine zipper is an appropriate nomenclature for parallel dimeric coiled coils (Landschultz *et al.*, 1988). The leucine zipper dimerization motif is critical for the functioning of two classes of DNA binding proteins: the bZIP (Vinson *et al.*, 1989) and bHLH-Zip proteins (Murre *et al.*, 1989).

The study of the essential structural elements that regulate leucine zipper dimerization stability and specificity has been facilitated by the fact that bZIP DNA binding is dependent on the correct dimerization of the leucine zipper structure. Several groups have shown that the hydrophobic core created by amino acids in the **a** and **d** position is critical for dimerization (Kouzarides and Ziff, 1988; Gentz *et al.*, 1989; Landschultz *et al.*, 1989; Turner and Tjian, 1989). As originally proposed by Landschultz *et al.* (1988), bZIP proteins not only homodimerize, but also heterodimerize via the leucine zipper structure (Hai *et al.*, 1989; Ivashkiv *et al.*, 1990; Roman *et al.*, 1990; Cao *et al.*, 1991; Hai and Curran, 1991; Williams *et al.*, 1991; Schindler *et al.*, 1992). However, only specific bZIP protein pairs can heterodimerize. Experiments using chimeric proteins and peptides indicate that all the structural information needed to regulate dimerization specificity is contained within the leucine zipper region (Agre *et al.*, 1989; Kouzarides and Ziff, 1989; O'Shea *et al.*, 1989).

The X-ray and NMR (Saudek *et al.*, 1991) structures of the GCN4 leucine zipper indicate that Crick's 'holes and knobs' description (Crick, 1953) of the dimer packing interface is a valid model. Amino acids in the **e** and **g** positions pack over the hydrophobic core created by the **a** and **d** positions, and possibly interact electrostatically. In the X-ray structure of the GCN4 leucine zipper (O'Shea *et al.*, 1991), GCN4 complexed to DNA (Ellenberger *et al.*, 1992; Konig and Richmond, 1993), and molecular dynamic calculations of the GCN4 zipper (Nilges and Brunger, 1991) interactions were observed between the **g** residue and the following **e** residue positioned five amino acids C-terminal on the opposite helix (denoted **e′**). Throughout this report, we refer to that interaction as the **g⟷e′** pair (when discussing a particular **g⟷e′** pair, the **g** and **e′** will be replaced by the relevant amino acid one-letter code). Several groups have implicated the amino acids in the **g** and **e** positions in the regulation of dimerization

specificity and stability (Nicklin and Casari, 1991; Schmidt-Dor *et al.*, 1991; Schuermann *et al.*, 1991; O'Shea *et al.*, 1992; Amati *et al.*, 1993; Loriaux *et al.*, 1993; Vinson *et al.*, 1993). Two groups (Hu *et al.*, 1993; Pu and Struhl, 1993) used a random mutagenesis approach to examine the significance of amino acids in the **g** and **e** position to dimer function and concluded that these positions are less important than the **a** and **d** positions for leucine zipper formation.

Work in this laboratory has shown that changing amino acids in the **g** and **e** positions of the homodimerizing bZIP protein C/EBP changes its dimerization properties (Vinson *et al.*, 1993). Proteins were generated that preferentially heterodimerized with wild-type C/EBP and are, therefore, potential dominant-negative proteins. Others were designed not to heterodimerize with C/EBP, but instead preferentially homodimerize. All these proteins were designed based on the assumption that E and R would create the most stabilizing **g**⟷**e′** pair. In order to proceed further with leucine zipper design, we needed quantitative information on the relative strengths of different **g**⟷**e′** pairs. The repeating nature of the leucine zipper structure suggests that design rules developed for a specific **g**⟷**e′** pair within a particular heptad can be used for any heptad, irrespective of their amino acid content. We expected the interaction energies to be additive over the length of the dimerization interface, a proposal supported by data from previously designed proteins (Vinson *et al.*, 1993).

A desire to understand the energetic rules governing leucine zipper dimerization stability and specificity has motivated our studies to determine the energetic contribution of pairs of amino acids on opposite sides of the structure. In this report, we present thermodynamic measurements of the energetic contribution of 27 systematic **g**⟷**e′** amino acid pairs to the thermal stability of the bZIP protein VBP (Iyer *et al.*, 1991), the chicken equivalent of the mammalian DBP (Mueller *et al.*, 1990). We have examined different combinations of six amino acids in the **e** and **g** positions: the four most common for these two positions, glutamic acid (E), glutamine (Q), arginine (R) and lysine (K), as well as aspartic acid (D) and alanine (A) (Vinson *et al.*, 1993). The dimerization stability of each new amino acid combination was determined using thermal melting monitored by circular dichroism (CD). These studies describe a thermodynamic scale for the stability of different **g**⟷**e′** amino acid pairs. The results produce protein design rules that can be used to modify leucine zipper-containing proteins to possess novel dimerization properties.

Results

The host bZIP protein: VBP (the chicken DBP)

The protein sequence of the first four leucine zipper heptads of the host or parental protein, the bZIP protein VBP (Iyer *et al.*, 1991), is presented in Figure 1B. The **g**⟷**e′** pairs immediately C-terminal to the DNA binding region are shown and numbered 1–4 depending on the heptad (defined here as **g,a,b,c,d,e,f**) within which they are found. The **g** position N-terminal of the first heptad interacts with DNA, as evidenced by the complex of GCN4 bZIP protein bound to DNA (Ellenberger *et al.*, 1992). Figure 1C presents a cartoon of a bZIP protein with the VBP amino acid sequence shown on a schematic of a coiled coil using the standard nomenclature for the seven unique amino acid positions

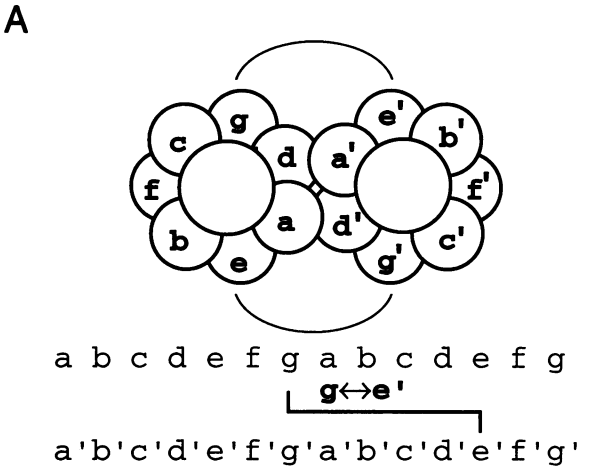

B

Heptad		1		2		3		4	
		g↔e'		g↔e'		g↔e'		g↔e'	
VBP	ITI	RAAF	LEK	ENTA	LRT	EVAE	LRK	EVGR	CKNI
coiled coil		gabcdef		gabcdef		gabcdef		gabcdefg	
E•R		R	E	E	R	E	R	E	R
E•K$_4$		R	E	E	R	E	R	E	K
E•K$_{34}$		R	E	E	R	E	K	E	K
E•K$_{1234}$		K	E	E	K	E	K	E	K
Q•E$_{1234}$		E	Q	Q	E	Q	E	Q	E

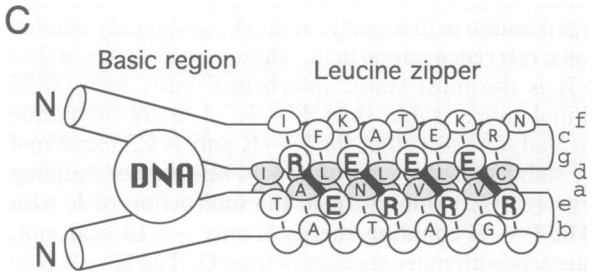

Fig. 1. (**A**) End view of a leucine zipper dimer looking from the N-terminus. The letters on the inside of each circle represent standard nomenclature for the seven amino acids found in unique positions in a coiled coil. Amino acids at the **a** and **d** positions create a hydrophobic core between the interacting helices. The interaction seen between amino acids in the **g** and subsequent **e′** position seen in X-ray structures is noted as **g**⟷**e′** pairs. (**B**) The amino acid sequence of the leucine zipper region of VBP, the chicken version of the mammalian DBP, is presented using the single-letter code. Below the VBP sequence is the nomenclature for the positions in a coiled coil. The sequence starts at the first 'leucine' position as defined previously (Vinson *et al.*, 1989) and is grouped into heptads (**g,a,b,c,d,e,f**). The leucine positions are italicized. The **g** to following **e′** (**g**⟷**e′**) pairs are denoted by bars above the potentially interacting amino acids that are highlighted in bold type face. The heptads are numbered 1–4. Note that because of the 2-fold symmetry of the dimers, each heptad contains two **g**⟷**e′** pairs. Amino acids in the **g** and **e** positions of representative mutant proteins are shown at the bottom of the figure to illustrate the nomenclature used. (**C**) The positions of the VBP leucine zipper amino acids seen on a schematic of a bZIP protein (Hu *et al.*, 1990) viewed from the side. Amino acids in the **e** and **g** position are shown in bold face. The heptad letter designations (**a,b,c,d,e,f,g**) are to the right of the figure. The supercoiling of the two helices is not depicted. To the left of the leucine zipper is the basic region of bZIP proteins with the DNA shown. The heptad N-terminal of heptad 1 has been shown to interact with DNA.

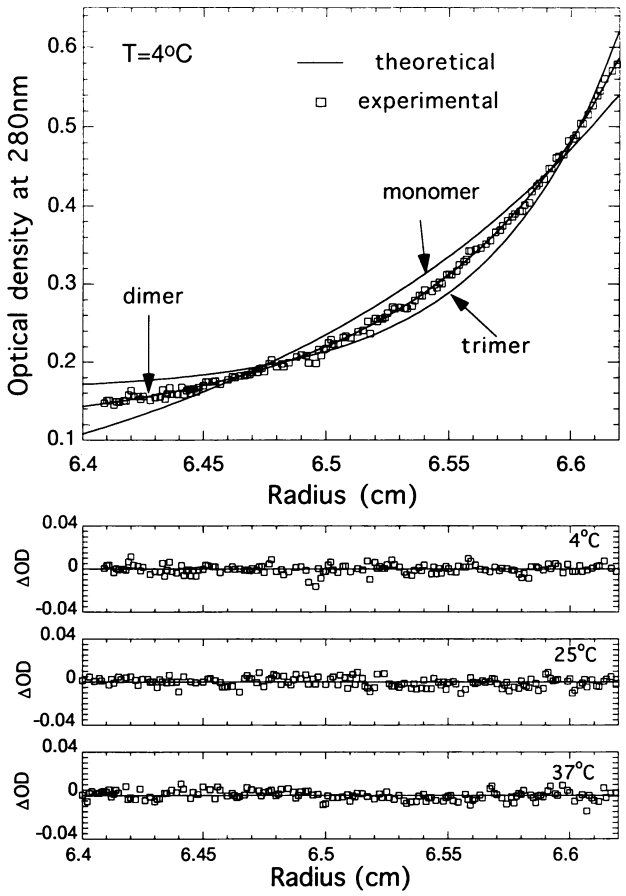

Fig. 2. Sedimentation equilibrium determination of the mol. wt of E·K_{1234} C-S at 4°C. The sample was in 12.5 mM potassium phosphate (pH 7.4), 150 mM KCl, 1 mM EDTA. Each sample was loaded at three concentrations (10, 20 and 40 μM) which have ODs of 0.1, 0.2 and 0.4 at 280 nm. Samples were spun at 25 000 r.p.m. for 24 h at 4°C. Theoretical curves for monomer, dimer or trimer are plotted as solid lines. The actual data are plotted as circles. These data clearly fit onto the dimer curve. The bottom panel shows the residual plots of fitting the experimental data to a monomer–dimer equilibrium model. No systematic error is evident.

(Hodges *et al.*, 1972). We chose to use VBP as the host molecule for three reasons. First, it is the only known bZIP protein which has the potential for attractive **g**⟷**e′** interactions at all four heptads, the most in any other protein is two. The most common attractive **g**⟷**e′** pair, found in the second, third and fourth heptads of VBP, has an acidic amino acid in the **g** position and a basic amino acid in the following **e** position (Vinson *et al.*, 1993). The first heptad has the opposite charge configuration (Figure 1B). The second reason for choosing this protein is that 8 of 12 charged amino acids in the leucine zipper region are in the **g** or **e** positions rather than in the **b**, **c** or **f** positions, thus potentially simplifying the electrostatic interactions on the coiled-coil surface. This contrasts with C/EBP, for example, where only 4 of 13 charged amino acids are in the **e** or **g** positions. The final reason for using VBP is the ease of overexpression in *Escherichia coli*.

The lower section of Figure 1B presents the nomenclature used to describe our various mutant proteins. All proteins are defined by two letters separated by a large period. Each letter represents the standard code for an amino acid in the relevant **g**⟷**e′** pair, the first letter being the amino acid in

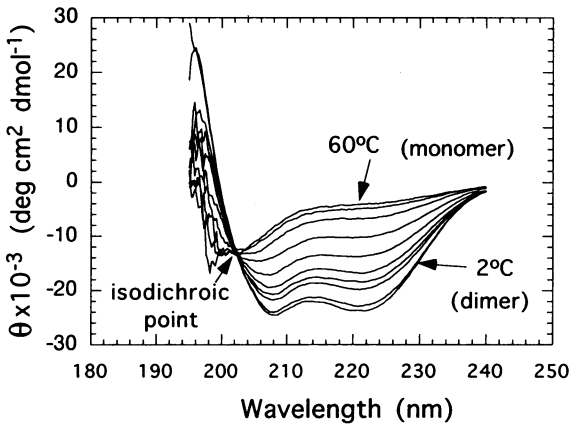

Fig. 3. Far-UV CD spectra of a 3.4 μM E·R sample as a function of temperature. The temperatures examined are from the highly ordered (dimer) to the random coil (monomer): 2, 6, 11, 20, 25, 30, 34, 40, 45, 45, 50 and 60°C. The minima at 208 and 222 nm are seen to disappear as the sample is heated. There is an isodichroic point at 202 nm. The sample was in 12.5 mM potassium phosphate (pH 7.4), 150 mM KCl, 1 mM EDTA.

the **g** position and the second letter the amino acid in the following **e** position. All proteins are defined relative to the protein E·R, where the second, third and fourth **g**⟷**e′** pairs are E⟷R, and the first pair is R⟷E. If a protein deviates from E·R, the **g**⟷**e′** pair which differs is identified. Thus, for example E·K_4, which is the original VBP protein, has R⟷E in the first heptad, E⟷R in the second and third heptads, and E⟷K in the fourth heptad. Several proteins have the cysteine replaced by serine and are referred to by the note C-S.

Sedimentation equilibrium of host bZIP protein

Gel-shift mixing experiments indicate that wild-type VBP binds DNA as a dimer (Vinson *et al.*, 1993). Sedimentation equilibrium data show that E·K_{1234} C-S behaves as a dimer at 4°C, even in the absence of DNA (Figure 2). At higher temperatures, 25 and 37°C, the sedimentation equilibrium data were fitted to a monomer–dimer equilibrium showing the temperature-induced dissociation of the dimer. Most of the mutant proteins to be discussed behaved as dimers at low temperatures.

Circular dichroism experiments of host bZIP protein: a simple two-state system

To determine whether or not helicity measured by CD would correlate with the extent of dimerization of the leucine zipper region observed by sedimentation equilibrium, we recorded far-UV CD spectra of a 3.4 μM solution of E·R as a function of temperature (Figure 3). The low-temperature spectra have minima at 208 and 222 nm, the signature for α-helices (Cooper and Woody, 1990). As the temperature is increased, these minima disappear, indicating the melting of the α-helical region. The presence of a clear isodichroic point (position common to all curves) is consistent with the two-state nature of the helix–random coil transition. Two-state melting was also observed recently for another bZIP protein, GCN4, in both CD and microcalorimetry studies (Thompson *et al.*, 1993). The thermal denaturation curves of our samples are reversible. Since VBP shows both reversible thermal

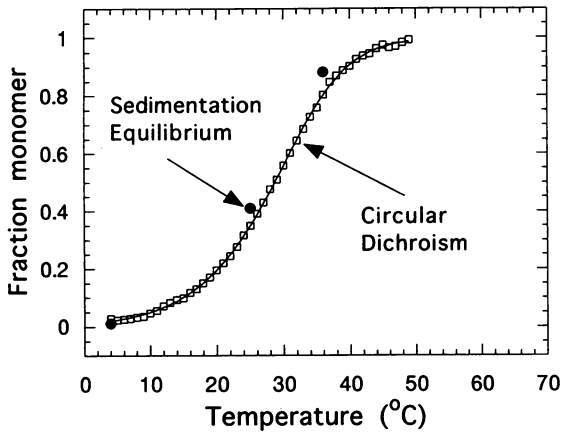

Fig. 4. The CD curve of E·K_{1234} C-S showing the fraction monomer as a function of temperature. The line through the data is a fitted curve as described in Materials and methods. Sedimentation equilibrium experiments were used to determine K_ds for the sample at 25 and 37°C. The K_ds obtained (2.4×10^{-5} M at 25°C and 5.5×10^{-3} M at 37°C) reflect a strong temperature dependence for dimerization. The K_d values were used to calculate the fraction monomer at the protein concentration used in the CD experiments and plotted at the respective temperatures as filled circles. The two methods of determining fraction monomer gave similar results.

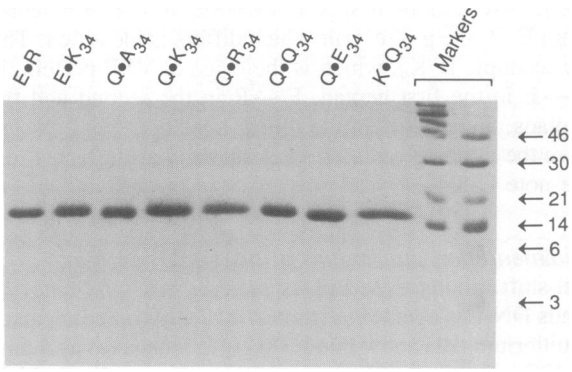

Fig. 5. Protein gel of eight purified proteins. Each protein is identified above the respective lane. We expressed and purified the mutant bZIP proteins from *E.coli* to >98% purity. Equal amounts of each protein, as determined spectroscopically, were loaded on a 14% SDS–polyacrylamide gel (Laemmli, 1970) and stained with Coomassie blue.

melting and a two-state transition upon thermal melting, thermodynamic parameters could be calculated (see Materials and methods).

The helicity, as measured by CD, was assumed to represent a two-state monomer–dimer equilibrium. The fraction monomer at different temperatures calculated from CD data was compared to the fraction monomer directly measured in the ultracentrifuge and found to be coincident (Figure 4). Thus, both CD measurements of helicity and sedimentation equilibrium measurements of molecular mass appear to monitor the same physical phenomenon: the melting of helical dimers into random coil monomers.

CD thermal denaturation was performed at different protein concentrations. The lowering of the melting temperature (T_m) at decreasing protein concentrations is consistent with the hypothesized monomer–dimer equilibrium (see Table I).

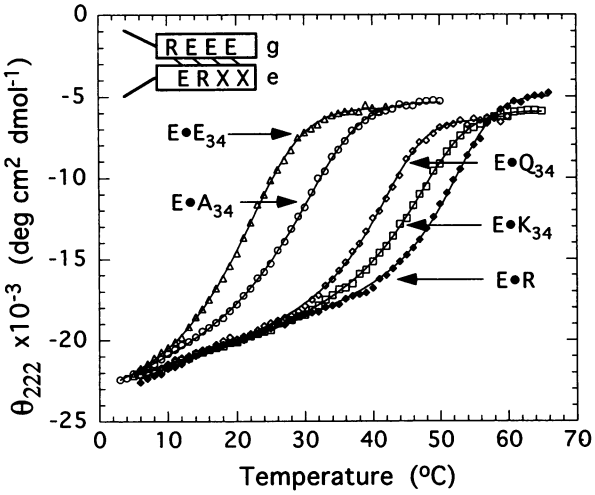

Fig. 6. CD thermal melting curves for the E·X_{34} proteins where X = A, R, K, Q or E. The line through each of the five labeled curves is a fitted curve as described in Materials and methods. Note that the initial baseline for each of the five curves is similar, indicating that all the samples start with the same fraction of dimer, which was shown to be 100% by sedimentation equilibrium. The cartoon in the upper left part of the figure is a graphic presentation of the **g** and **e′** amino acid identities, and the presumed interactions are indicated by a line connecting the amino acids.

Thermodynamic stability of different g⟷e′ pairs

We generated a large collection of proteins mutated in the **g** and **e′** positions. The energetics of the structurally observed **g⟷e′** interactions were calculated based on the fact that our host protein exhibited a simple two-state transition upon thermal denaturation. The aim was to generate protein design rules based on a thermodynamic scale for various **g⟷e′** amino acid pairs. Examination of the **e** and **g** positions of bZIP proteins shows that >80% of these positions are occupied by only four amino acids (Vinson *et al.*, 1993): K, R, E and Q. These represent three of the four charged amino acids and, perhaps more importantly, they contain long hydrophobic side chains. This may be essential for hydrophobic packing over the hydrophobic core created by the **a** and **d** positions (O'Shea *et al.*, 1991).

Six amino acids in the **g** and following **e** positions were systematically varied, namely the four commonly occurring amino acids in these positions, K, R, Q and E, as well as the only other remaining charged amino acid D, and finally A, a truncated amino acid used as a reference. Amino acids were changed in the fourth pair (two proteins), the third and fourth pairs (25 proteins), and the first, second, third and fourth pairs (six proteins). Figure 5 shows a representative protein gel of a number of the proteins purified from *E.coli*. All proteins were similarly pure.

The raw CD data for the thermal melting of five different E·X_{34} proteins are seen in Figure 6. In these samples mutated in the third and fourth **g⟷e′** pairs, the **g** position is always occupied by E, while the **e** position is occupied by X = A, R, K, Q or E. All five samples have the same molar ellipticity at low temperatures, suggesting that each is totally dimeric at the beginning of the thermal melting, an assertion supported by ultracentrifugation data. At low temperatures, all five samples show a similar initial CD linear baseline followed by a clear co-operative transition indicative of melting of the helical leucine zipper. After thermal denaturation, all samples again have a similar

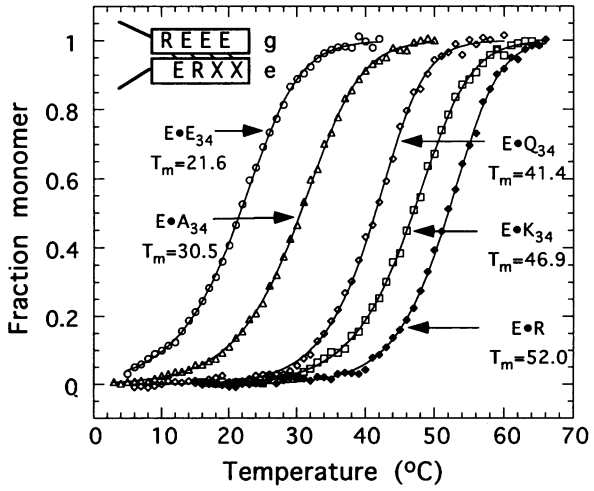

Fig. 7. The data from Figure 6 replotted as fraction monomer. The line through each curve is a fitted curve. The T_m for each of the five curves is noted.

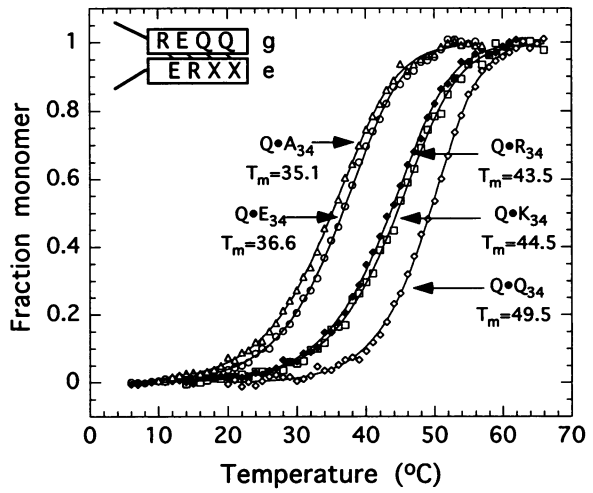

Fig. 8. CD thermal melts for $Q \cdot X_{34}$ proteins where X = A, R, K, Q or E, plotted as fraction monomer. The line through each curve is a fitted curve. The T_m for each of the five curves is noted. Note that the curves are more clustered and shifted toward the higher temperatures relative to Figure 7.

ellipticity. The same data plotted in terms of fraction monomer are shown in Figure 7. There is a 30°C difference in melting temperature (T_m) between the most ($E \cdot R$) and least ($E \cdot E_{34}$) stable sample. $E \cdot R$ is more stable than $E \cdot K_{34}$. Both $E \cdot R$ and $E \cdot K_{34}$ have similar interacting charges, but their relative stability is as different as that between $E \cdot K_{34}$ and $E \cdot Q_{34}$ which have no charge−charge attraction.

CD data were obtained for the thermal melting of five different $Q \cdot X_{34}$ proteins mutated in the third and fourth heptads where the **g** position was always occupied by Q, but the **e** position was again occupied by the same amino acids used previously, X = A, R, K, Q or E (Figure 8). There is only a 15°C difference in the T_ms between the most ($Q \cdot Q_{34}$) and least ($Q \cdot A_{34}$) stable samples. Q interacts more stably with the basic amino acids, K and R, than with the acidic amino acid E.

Table I presents thermodynamic parameters calculated from CD thermal melts for 33 proteins that have been systematically varied to reveal the energetics of different **g**⟷**e′** pairs. Each of the samples examined have different melting temperatures, indicating that changing amino acids in the **g** and **e** positions affects protein stability. Most samples retained their dimeric properties. The free energy differences due to mutations of E⟷R pairs to other **g**⟷**e′** pairs were calculated from the difference in stability between $E \cdot R$ and mutant proteins. Mixing of two different proteins can create heterodimers with novel **g**⟷**e′** pairs, which have been included in Table I. For example, the $E \cdot E_{34}/R \cdot R_{34}$ heterodimer contains both E⟷R and R⟷E pairs. The difference between the E⟷R homodimer and $E \cdot E_{34}/R \cdot R_{34}$ heterodimer is the replacement of two E⟷R with two R⟷E pairs. Thus, the difference in stability between these two dimers is the energetic difference between the E⟷R and R⟷E pair. This allows the calculation of the energy contribution of a R⟷E pair to stability.

The generality of the stability of **g**⟷**e′** pairs ($\Delta\Delta G$) calculated from molecules mutated in the third and fourth heptads was addressed by creating proteins with changes in either only the fourth pair or all four pairs (Figure 9). The results show that, except for Q⟷Q, the calculated $\Delta\Delta G$ values per **g**⟷**e′** pair are nearly independent of the heptad within which they reside.

Stability of g⟷e′ pairs relative to A⟷A

Table II presents a matrix of **g**⟷**e′** pair stability for all combinations of amino acids investigated. The $\Delta\Delta G_{E \cdot R}$ values, found in Table I, for proteins containing altered third and fourth **g**⟷**e′** pairs were recalculated relative to A⟷A. The A⟷A pair was chosen as the baseline because A is a truncated amino acid. A is unable to interact with its partner in a **g**⟷**e′** pair since the β-carbons of the **g**⟷**e′** pairs are 9 Å apart, in fact the presence of a single A precludes **g**⟷**e′** interactions (O'Shea *et al.*, 1991). The most appropriate control protein, $A \cdot A_{34}$, was insoluble. $A \cdot A_4$, however, is soluble and has an interpretable CD thermal denaturation profile [$A \cdot A_3$ was insoluble in low salt, but not high (1 M KCl) salt]. Since thermodynamic parameters were calculated per **g**⟷**e′** pair, $A \cdot A_4$ could be used to determine a reference point for $\Delta\Delta G$.

Because of the importance of the energetic value of the A⟷A pair in subsequent calculations of coupling energies between amino acids in the **g**⟷**e′** pair, we independently calculated the value of the A⟷A pair using two mixing experiments. A mixture of $E \cdot A_{34}$ and $A \cdot R_{34}$ formed a heterodimer, as evidenced by the one-stage melting transition with a T_m higher than either homodimer. The structural difference between this heterodimer and the $E \cdot R$ homodimer is the replacement of an E⟷R pair in both the third and fourth heptad with A⟷A pairs. The difference in ΔG_o between an $E \cdot A_{34}/A \cdot R_{34}$ heterodimer and $E \cdot R$ homodimer of 2.82 kcal/mol is a measure of the strength of an A⟷A pair relative to an E⟷R pair in both the third and fourth heptads. The average value of 1.41 kcal/mol/pair is similar to the value of 1.33 calculated for the A⟷A pair from $A \cdot A_4$. A similar type of experiment examined the difference in ΔG_o between the heterodimer $A \cdot E_{34}/R \cdot A_{34}$ and $E \cdot E_{34}/R \cdot R_{34}$ which again differ by an A⟷A pair in both the third and fourth heptad. This analysis suggests that A⟷A is 1.46 kcal/mol less stable than E⟷R. The similarity between the values obtained for the A⟷A pair by melting $A \cdot A_4$ and the two heterodimers containing A⟷A pairs gave us a greater confidence in the calculation of the energetic strength of the A⟷A pair.

Table I. Fitted thermodynamic parameters calculated for the thermal unfolding of different VBP g⟷e′ derivatives per mole of dimer

Sample 3.4 μM	T_m (°C)	$\Delta H(T_m)$ (kcal/mol)	$\Delta G(37)$ (kcal/mol)	$\Delta\Delta G_{E\cdot R}$ (kcal/mol)	$K_d(37)$ (mol)	Mw[a] (kDa)
E·R	52.0 ± 0.1	−83	−11.2	0.00	1.4e-08	21.9
EK_4	49.7 ± 0.1	−74	−10.4	0.40	5.2e-08	
$Q\cdot Q_{34}$	49.3 ± 0.2	−80	−10.6	0.16	3.9e-08	21.7
$E\cdot K_{34}$	47.0 ± 0.1	−70	−9.80	0.35	1.4e-07	
$Q\cdot K_{34}$	44.5 ± 0.2	−63	−9.18	0.50	3.7e-07	21.8
$Q\cdot R_{34}$	43.5 ± 0.1	−64	−9.04	0.54	4.7e-07	22.5
$E\cdot K_{1234}$	42.3 ± 0.2	−67	−8.87	0.29	6.1e-07	21.6
$A\cdot Q_{34}$	42.0 ± 0.1	−71	−8.88	0.58	6.0e-07	
$K\cdot Q_{34}$	41.9 ± 0.2	−61	−8.70	0.62	8.0e-07	22.1
$E\cdot Q_{34}$	41.3 ± 0.1	−77	−8.82	0.60	6.6e-07	18.8
$A\cdot K_{34}$	41.3 ± 0.2	−68	−8.70	0.63	8.1e-07	21.1
$A\cdot A_4$	40.3 ± 0.2	−73	−8.55	1.33	1.0e-06	21.6
$R\cdot Q_{34}$	38.9 ± 0.2	−65	−8.19	0.75	1.8e-06	
$Q\cdot E_{34}$	36.6 ± 0.2	−63	−7.72	0.87	3.9e-06	22.6
$Q\cdot A_{34}$	35.1 ± 0.3	−58	−7.44	0.94	6.2e-06	20.2
$Q\cdot R_{1234}$	35.0 ± 0.2	−64	−7.38	0.48	6.8e-06	
$Q\cdot K_{1234}$	34.0 ± 0.2	−62	−7.18	0.50	9.4e-06	
$K\cdot K_{34}$	33.4 ± 0.8	−45	−7.25	0.99	8.4e-06	
$A\cdot E_{34}$	33.0 ± 0.2	−63	−6.95	1.1	1.4e-05	17.3
$K\cdot R_{34}$	33.0 ± 0.2	−47	−7.16	1.0	9.7e-06	
$Q\cdot Q_{1234}$	32.8 ± 0.2	−56	−7.00	0.53	1.3e-05	18.9
$K\cdot A_{34}$	31.5 ± 0.2	−51	−6.84	1.09	1.6e-05	
$R\cdot A_{34}$	30.7 ± 0.2	−49	−6.71	1.12	2.0e-05	20.9
$E\cdot A_{34}$	30.5 ± 0.2	−60	−6.43	1.19	3.1e-05	21.2
$R\cdot R_{34}$	27.1 ± 0.4	−40	−6.29	1.23	3.9e-05	
$R\cdot K_{34}$	26.2 ± 0.8	−37	−6.24	1.24	4.2e-05	
$A\cdot R_{34}$	25.3 ± 0.8	−37	−6.09	1.28	5.5e-05	22.5
$E\cdot E_{34}$	21.6 ± 0.4	−56	−4.41	1.70	8.1e-04	21.1
$E\cdot Q_{1234}$	20.6 ± 0.5	−50	−4.49	0.84	7.2e-04	
$D\cdot R_{34}$	17.5 ± 1.5	−40	−4.37	1.71	8.7e-04	
$D\cdot A_{34}$	<0.00	(−40)[b]	0.41	>2.90	1.9e + 00	
$D\cdot D_{34}$	<0.00					
$D\cdot K_{34}$	15.5 ± 0.5	−47	−3.39	1.95	4.2e-03	
$Q\cdot A_{1234}$	21.7 ± 1.5					36.7[c] (26.3)
E·R C-S	40.6 ± 0.2	−71	−8.59		9.6e-07	21.8
$E\cdot K_{1234}$ C-S	30.1 ± 0.2	−44	−6.71		2.0e-05	21.3
$E\cdot K_4$ (1 μM)	44.9 ± 0.3	−74	−10.3	0.46	6.3e-08	
$E\cdot K_4$ (8.2 μM)	51.6 ± 0.1	−78	−10.4	0.41	5.4e-08	
$E\cdot K_4$ (27.5 μM)	54.6 ± 0.1	−82	−10.4	0.43	5.6e-08	
$E\cdot E_{34}/RK_{34}$	50.3 ± 0.1	−80	−11.2		1.4e-08	
$A\cdot E_{34}/RA_{34}$	41.5 ± 0.2	−68	−8.74		7.6e-07	21.6
$E\cdot A_{34}/AR_{34}$	39.9 ± 0.2	−63	−8.37		1.4e-06	
$E\cdot E_{34}/KR_{34}$	50.6 ± 0.1	−83	−11.4		1.1e-08	
$E\cdot E_{34}/RR_{34}$	51.5 ± 0.1	−85	−11.6		7.0e-09	

The table presents energetic calculations for a variety of mutant VBP proteins. The following parameters are presented: melting temperature, T_m and curve fitting error; dimerization free energy extrapolated to T = 37°C, $\Delta G(37)$; dimerization van't Hoff enthalpy at $T = T_m$, $\Delta H(T_m)$; dissociation constant at 37°C, $K_d(37)$; the mol. wt as determined by sedimentation equilibrium, Mw; the energetic difference in a single g⟷e′ pair relative to E⟷R, $\Delta\Delta G_{E\cdot R}$. Samples are arranged in order of decreasing thermal stability of the non-covalently linked protein. All the samples reported here have a similar ellipticity at low temperatures, suggesting that they are dimeric before thermal denaturation. The standard errors for ΔG_o vary from ±0.04 to ±0.16 kcal/mol, except for $D\cdot R_{34}$ (0.38 kcal/mol).

[a]The mol. wt (Mw) of the E·R monomer is 11 256 Da.

[b]ΔH was assumed to allow a calculation of ΔG.

[c]This sample fits a monomer−tetramer equilibrium equation. The value in parentheses is for the oxidized sample.

Coupling energies ($\Delta\Delta G_{int}$) of g⟷e′ pairs

The data described so far do not demonstrate that the calculated differences in energy are necessarily caused by the interaction of amino acids in the **e** and **g** positions. These differences could simply be the sum of the independent energetic contributions of each amino acid in the g⟷e′ pair. Evidence for an interaction between amino acids in g⟷e′ pairs was obtained from two arguments. The first is based on a thermodynamic cycle and the second is from mixing experiments discussed in the next section. A thermodynamic cycle required the generation of proteins with non-interacting g⟷e′ pairs. We generated a set of proteins with A in either the **e**, **g**, or **e** and **g** positions, e.g. $E\cdot A_{34}$, $A\cdot R_{34}$ and $A\cdot A_4$. By comparing the stability of these proteins with proteins in which the **e** and **g** positions are occupied by potentially interacting amino acids, e.g. E·R, we were able to calculate an energy of interaction between E and R, termed the coupling energy ($\Delta\Delta G_{int}$).

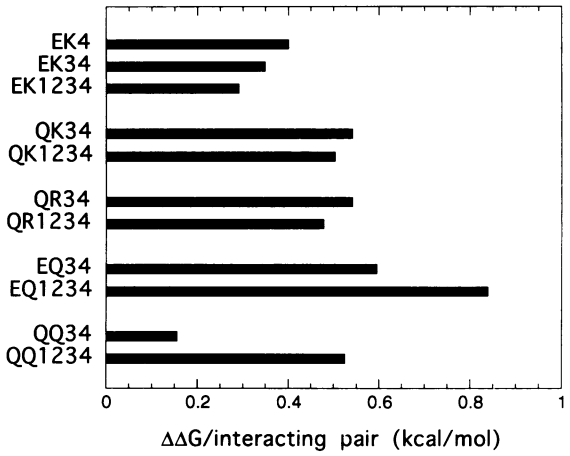

Fig. 9. Histogram of the calculated energetic strength of different **g**⟷**e′** pairs relative to E⟷R ($\Delta\Delta G_{E\cdot R}$) for proteins with different numbers of a particular **g**⟷**e′** pair. The top of the figure shows three proteins containing one, two or four E⟷K pairs. The average difference in stability is consistently around 0.4 kcal/mol relative to E⟷R, suggesting that the measured difference is independent of the location of the particular **g**⟷**e′** pair along the length of the leucine zipper. Note that in the constructs that contain an altered first heptad, the order of the amino acid pair is reversed, as is true for the host protein. The general conclusion is that the calculated stability of a particular **g**⟷**e′** pair is similar for proteins in which all four heptads have the same amino acid pair or only the third and fourth heptads have the same pair. The one notable exception is Q⟷Q; $Q\cdot Q_{34}$ is very stable, while $Q\cdot Q_{1234}$ is much less stable than expected, suggesting that some particular structural interaction is occurring in one context, but not the other.

Table II. Thermodynamic differences for **g**⟷**e′** interactions relative to A⟷A ($\Delta\Delta G_{A\cdot A}$) (kcal/mol)

↓g/e′→	A	E	Q	R	K
A	0.0	−0.27	−0.75	−0.05	−0.70
E	−0.14	+0.37	−0.73	−1.33	−0.98
Q	−0.39	−0.46	−1.17	−0.79	−0.83
R	−0.21	−1.55[a]	−0.58	−0.10	−0.10
K	−0.24	−1.42[a]	−0.71	−0.32	−0.34
D	>+1.57	–	–	+0.38	+0.62

The $\Delta\Delta G_{E\cdot R}$ values from Table I were recalculated relative to the A⟷A pair to produce $\Delta\Delta G_{A\cdot A}$. The standard errors for $\Delta\Delta G_0$ vary from ±0.01 to ±0.04 kcal/mol except for $D\cdot R_{34}$ (0.1 kcal/mol).
[a]The R⟷E and K⟷E values were calculated from the melting of heterodimers (see Table I).

A thermodynamic cycle for the E⟷R pair is presented in Figure 10. As noted earlier, the E⟷R pair is −1.33 kcal/mol more stable than A⟷A. To determine the coupling energy ($\Delta\Delta G_{int}$) between E and R, the independent contributions of either E or R alone to the stability of the leucine zipper had to be determined. This was accomplished by examining the stability of $E\cdot A_{34}$ and $A\cdot R_{34}$. The difference in stability between an A⟷A pair and other A-containing pairs (e.g. A⟷R) shows the ability of the non-alanine amino acid to stabilize the dimer independently of a **g**⟷**e′** interaction. The E⟷A pair is −0.14 kcal/mol more stable than A⟷A and the A⟷R pair is −0.05 kcal/mol more stable than A⟷A. Subtracting these values from the measured −1.33 kcal/mol for the E⟷R pair gives a value of −1.14 kcal/mol for the coupling energy ($\Delta\Delta G_{int}$) of E interacting with R.

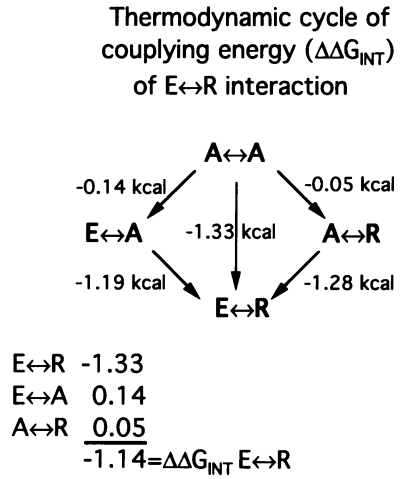

Fig. 10. Thermodynamic cycle for the interaction of glutamic acid in the **g** position with arginine in the following **e′** position. The four proteins in the cycle are $A\cdot A_4$, $E\cdot A_{34}$, $A\cdot R_{34}$ and E·R. The $\Delta\Delta G$ values presented are in terms of an individual **g**⟷**e′** interaction. The E⟷R pair is 1.33 kcal/mol more stable than A⟷A. The contribution of the individual amino acids to the stability of the leucine zipper was determined by studying $E\cdot A_{34}$ and $A\cdot R_{34}$. The E⟷A pair is 0.14 kcal/mol more stable than A⟷A. The A⟷R pair is 0.05 kcal/mol more stable than A⟷A. The sum of the individual contributions of E and R to the dimer stability is −0.19 kcal/mol. The extra −1.14 kcal/mol of stability [−1.33−(−0.19)] from the E⟷R pair is the coupling energy (ΔG_{int}) indicative of the interaction of E with R across the leucine zipper.

Table III. Coupling energy ($\Delta\Delta G_{int}$) of **g**⟷**e′** pair (kcal/mol)

↓g/e′→	E	Q	R	K
E	+0.78	+0.16	−1.14	−0.14
Q	+0.20	−0.03	−0.35	+0.26
R	−1.07[a]	+0.38	+0.16	+0.81
K	−0.91[a]	+0.28	−0.03	+0.60

The coupling energy ($\Delta\Delta G_{int}$) was calculated from values given in Table II. The $\Delta\Delta G$ values for both the X⟷A and A⟷Y pairs were subtracted from the value for the X⟷Y pair to determine the X⟷Y coupling energy ($\Delta\Delta G_{int}$).
[a]as Table II.

Coupling energies for 16 **g**⟷**e′** pairs are presented in Table III. In contrast to the E⟷R pair, the E⟷K pair shows a negligible coupling energy of −0.14 kcal/mol. A general trend from these coupling energy calculations is that **g**⟷**e′** pairs containing R in the **e** position have stronger (more negative) coupling energies than those containing K in the **e** position. An observation that was not expected from model building is the large number of positive coupling energies. These suggest that there is some sort of repulsion or steric clash between amino acids trying to occupy the same hydrophobic patch over the leucine zipper core. The order of amino acids in the **g**⟷**e′** pair also affects the coupling energy. For example, K⟷R shows a negligible coupling energy of −0.03 kcal/mol, while R⟷K shows the strongest measured repulsive coupling energy of +0.81 kcal/mol. This difference suggests that the order of amino acids in a **g**⟷**e′** pair is critical for the amino acid interactions. The order-dependent coupling energy is not seen for all **g**⟷**e′** pairs, the K⟷Q and Q⟷K pairs have a similar coupling energy of +0.27 kcal/mol.

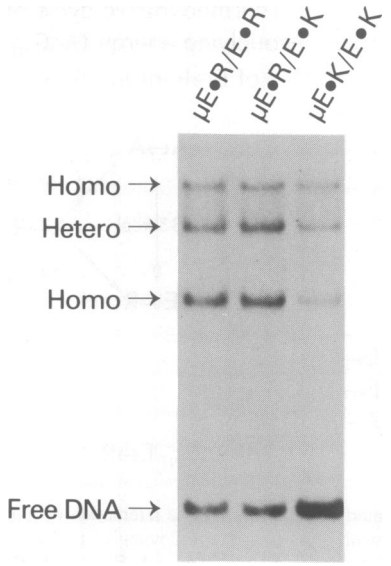

Fig. 11. Gel-retardation assay mixing two different size proteins. Equal moles of the four proteins named in the figure were mixed as indicated. Note that the mixing of $\mu E \cdot R$ with $E \cdot K_{1234}$ results in a similar proportion of heterodimer formed as in either the $\mu E \cdot R$ with $E \cdot R$ or $\mu E \cdot K_{1234}$ with $E \cdot K_{1234}$. $\mu E \cdot R$ binds DNA about twice as well as $E \cdot R$ which explains the greater DNA shifting of $\mu E \cdot R$ relative to $E \cdot R$. Also, $E \cdot K_{1234}$ binds DNA less well than $E \cdot R$.

Novel heterologous interactions regulate dimerization specificity

Amino acids in the **g** and **e** positions have been implicated in regulating dimerization specificity. Since the mutant proteins described here involve changes only in these positions, they were used in mixing experiments to investigate the specificity of hetero versus homodimerization. If we mixed $E \cdot R$ and $E \cdot K_{1234}$, the heterodimer would contain an equal number of E⟷R and E⟷K interactions which are the same type of interactions present in the respective homodimers. A thermodynamic analysis, assuming **g**⟷**e**′ pairs are independent of each other, reveals that the stability of the heterodimer would be the average of the stabilities of the two homodimers. This suggestion was tested using a gel-shift assay. A short version of the protein $E \cdot R$ was independently mixed with two proteins, a large $E \cdot R$ and a large $E \cdot K_{1234}$, bound to DNA and resolved on a native polyacrylamide gel (Figure 11). The formation of heterodimer is similar in all three lanes. The $E \cdot R/E \cdot K_{1234}$ heterodimer contains an equal number of E⟷R and E⟷K interactions, and consequently would be expected to be intermediate in stability between $E \cdot R$ and $E \cdot K_{1234}$, 1.2 kcal/mol less stable than $E \cdot R$. One might have expected that mixing of $E \cdot R$ with a protein 2.3 kcal/mol less stable ($E \cdot K_{1234}$) would result in less formation of heterodimers. This is not the result; the laws of mass action allow a less stable protein ($E \cdot K_{1234}$) to disrupt the stability of a more stable protein ($E \cdot R$) if the heterodimer is of intermediate stability.

In the second mixing experiment, the stability of the heterodimer is calculated to be greater than the average of the two homodimer stabilities, thus favoring the formation of heterodimers. Mixing E⟷E and R⟷R would result in a heterodimer containing E⟷R and R⟷E interactions which are not present in the homodimers. Two proteins

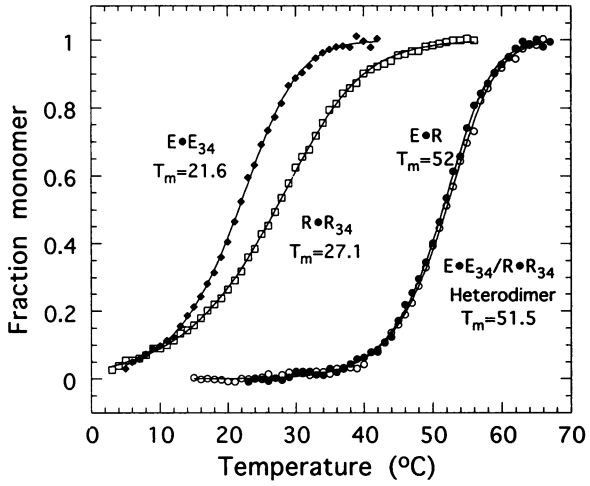

Fig. 12. Mixing of $E \cdot E_{34}$ with $R \cdot R_{34}$. This plot shows the CD thermal melting of four samples as labeled. They are $E \cdot E_{34}$, $R \cdot R_{34}$, $E \cdot R$, and an equimolar mixture of $E \cdot E_{34}$ with $R \cdot R_{34}$. The equimolar mixture of $E \cdot E_{34}$ and $R \cdot R_{34}$ melts as a single stable species, much more stable than either alone, suggesting that these proteins form heterodimers. The presumed $E \cdot E_{34}/R \cdot R_{34}$ heterodimer has a melting profile similar to $E \cdot R$. The total protein concentration for all samples was 3.4 μM.

($E \cdot E_{34}$ and $R \cdot R_{34}$) were mixed and shown to be more thermally stable than solutions of either protein alone (Figure 12) (Graddis *et al.*, 1993; O'Shea *et al.*, 1993). In fact, the mixture of $E \cdot E_{34}$ and $R \cdot R_{34}$ has similar stability to $E \cdot R$. We argue that the increased stability comes from the novel pair of amino acids in the **g** and **e** position present only in the heterodimer. The interaction could be either attractive between dissimilar monomers, encouraging heterodimers, or due to repulsion between similar monomers discouraging homodimers, or a combination of both.

A in the e position can create tetramers

Eighteen mutant proteins were analyzed in the analytical ultracentrifuge, at temperatures below the transition temperature, to determine their oligomerization properties. Most are dimers with surprisingly small variations in the calculated mol. wts. $Q \cdot A_{1234}$, however, did show a dramatic change in mol. wt. Analysis of sedimentation data revealed that this molecule behaves as a tetramer (Figure 13). However, $Q \cdot A_{34}$, a similar protein to $Q \cdot A_{1234}$, behaves as a dimer. It is likely that the conversion to tetramer is caused by the large hydrophobic face present in $Q \cdot A_{1234}$. Oxidized $Q \cdot A_{1234}$, corresponding to a covalently linked leucine zipper, is dimeric, while the reduced $Q \cdot A_{1234}$ sample is tetrameric. This indicates that the tetramer is not two interacting leucine zipper dimers. Similarly, the **e** and **g** positions of the GCN4 leucine zipper have been mutated to A, attached to a DNA binding domain and found to form tetramers (Alberti *et al.*, 1993).

Discussion

This paper reports the thermal stability of 33 leucine zipper proteins containing 27 different systematic combinations of amino acids in the **g** position on one helix and the following **e** position on the opposite helix (denoted **g**⟷**e**′). CD thermal stability measurements have allowed us to determine the

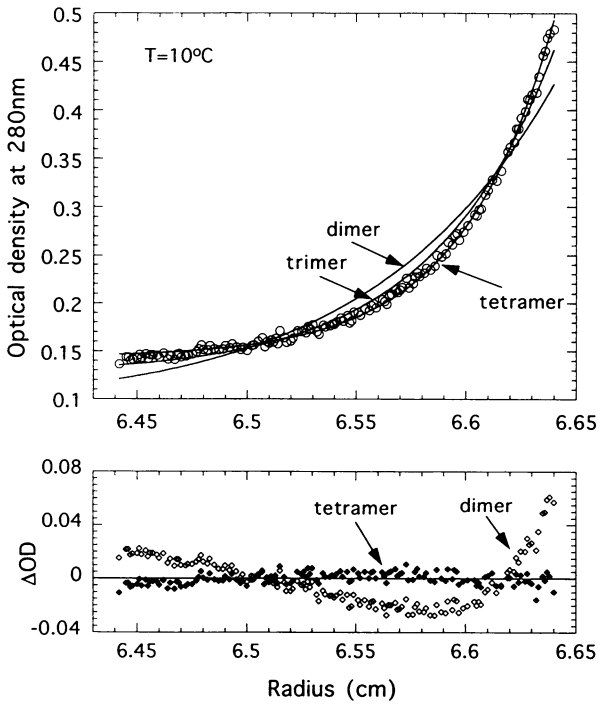

Fig. 13. Sedimentation equilibrium determination of the mol. wt of $Q \cdot A_{1234}$ at 10°C. The sample was in 12.5 mM potassium phosphate (pH 7.4), 150 mM KCl, 1 mM EDTA, 1 mM DTT. Each sample was loaded at three concentrations (10, 20 and 40 μM) which have ODs of 0.1, 0.2 and 0.4 at 280 nm. Samples were spun at 25 000 r.p.m. for 24 h. Theoretical curves for a dimer, trimer and tetramer are plotted as solid lines. The actual data are plotted as circles. These data clearly fit onto the tetramer curve. The bottom panel shows the residual plots of fitting the experimental data to a dimer model or tetramer model. The tetramer model shows less systematic error in the residual plot, indicating that it fits the data better. If the sample was prepared and spun in the absence of DTT, the data obtained fitted a dimer curve.

energetic contribution of a single **g**⟷**e′** amino acid pair and, based on a thermodynamic cycle analysis, formally determine the coupling energy ($\Delta\Delta G_{int}$) between the amino acids in **g**⟷**e′** pairs. The results have provided some general rules concerning **g**⟷**e′** pairs. E⟷R is the most stable **g**⟷**e′** pair. R has a wider range of dimerization stabilities than K, suggesting more potential for specificity in leucine zipper dimerization. E has a wider range of dimerization stabilities than Q, which generally forms stable **g**⟷**e′** pairs even though it is uncharged. These rules should allow the design of leucine zipper proteins that would specifically dimerize with target leucine zipper helices, but not with others.

ΔΔG of g⟷e′ pairs is position independent

An important concern in these experiments is whether or not the **g**⟷**e′** pairs studied were energetically independent of the rest of the leucine zipper structure. It could be argued that each heptad is structurally unique, and only a well-defined heptad should be studied. We took an alternative approach of examining **e** and **g** pairs in different structural environments, and taking an average in the hope of producing more general design rules. Additionally, we wanted to amplify any change in stability by changing **g**⟷**e′** pairs in two different heptads, which represents four interactions: two interactions per heptad, one on each side of the leucine zipper. Examination of the third and fourth heptads of VBP (Figure 1) shows that besides the charged amino acids in the **g** and **e** positions, charged amino acids are also present in the **c** position. The third heptad has an E and the fourth heptad has an R. Work by several groups has shown that intrahelical salt bridges, both (i,i + 3) and (i,i + 4), can exist. Thus, the possibility exists of a (i,i + 3) type intrahelical salt bridge existing between the **g** and following **c** position in both the third and fourth heptad (Marqusee and Baldwin, 1987; Fairman *et al.*, 1990; Gans *et al.*, 1991; Scholtz *et al.*, 1993). Fortunately, the **c** amino acids in the third and fourth heptads are of opposite charge, hopefully canceling out any systematic error in these experiments caused by the **c** amino acids having the same charge. The crystal structure of the leucine zipper protein, GCN4, shows that E(270) in the **g** position appears to form a **g**⟷**e′** interhelical interaction with K(275), and an (i,i + 3) intrahelical interaction with R(273). This observation suggests that the thermal stability being measured may be a complex combination of interactions between the **g** and the following **c** and **e′** positions.

To determine if the **g**⟷**e′** pairs examined were acting independently of the local leucine zipper structure, we examined proteins containing different numbers of a particular **g**⟷**e′** pair and determined the average strength of each pair. In most cases, similar $\Delta\Delta G$ values per **g**⟷**e′** pair were obtained for each of five different **g**⟷**e′** pairs present in one, two or four repeats. Since the **g** and **e** amino acids pack over the hydrophobic core, particularly the **a** position (O'Shea *et al.*, 1991), the identity of the amino acid in the **a** position may influence the energetics of the **g**⟷**e′** interaction. The results presented in Figure 9 support the general conclusion that the $\Delta\Delta G$ values per **g**⟷**e′** pair are independent of position along the leucine zipper, even though the first and second heptads have an alanine and asparagine, respectively, in the **a** position, while the third and fourth heptads have a valine. This suggests that the contribution of the **a** position to **g**⟷**e′** pair stability is not dramatic. The only exception to this result is Q⟷Q. The $Q \cdot Q_{34}$ protein indicates that Q⟷Q is much stronger than anticipated from examination of $Q \cdot Q_{1234}$. We do not know if these results over- or under-represent the actual Q⟷Q interaction energy. No simple interpretation of this result is obvious.

Stabilizing contributions of amino acids in the e or g positions

The contribution of individual amino acids in the **e** and **g** positions to the formation of leucine zippers can be conceptually divided into three distinct effects: oligomerization state, inherent dimer propensity and dimerization specificity. The first effect is the propensity to form different oligomeric states. Muller-Hill's group has shown that changing amino acids in the **e** and **g** positions switches the oligomerization between dimers and tetramers (Alberti *et al.*, 1993). Our own work with the protein $Q \cdot A_{1234}$ has shown that placing an A in each of the four **e** positions can create tetramers.

The second contribution of amino acids in the **e** and **g** positions is the inherent propensity of a particular amino acid to form a dimeric coiled coil. This is analogous to the α-helix-forming propensities of amino acids for isolated α-helices (Lye *et al.*, 1990; Padmanabhan *et al.*, 1990; Blaber

et al., 1993) and solvent-exposed positions (the **f** position) of a coiled coil (O'Neil and DeGrado, 1990). The stability of A⟷X- or X⟷A-containing proteins allows the determination of the energetic contribution of the X amino acid in either the **g** or **e** position in presumed isolation from any **g**⟷**e′** interaction. These stabilities could reflect the α-helical propensity of a particular amino acid. The difference between the α-helical propensity of a particular amino acid and our data for the **e** and **g** positions reflects the structural consequence of these two positions being near the hydrophobic interface of the leucine zipper. For example, A⟷K is 0.70 kcal/mol more stable than A⟷A even though K forms helices 0.12 kcal/mol more poorly than A (O'Neil and DeGrado, 1990). This difference of 0.82 kcal/mol reflects the ability of K in the **e** position to stabilize the leucine zipper independent of α-helix propensity. This is probably due to the methylenes of the lysine side chain packing over the hydrophobic core of the leucine zipper. Similar, though less dramatic, results are seen with the amino acids E, Q and R, all of which have long side chains. However, aspartic acid forms helices 0.62 kcal/mol more poorly than A, but in the **g** position is >1.5 kcal/mol less stabilizing than A. This additional destabilization of D in the **g** position suggests that the short side chain of D may cause destabilization greater than expected based on α-helical propensity.

Calculating the strength of a **g**⟷**e′** pair relative to A⟷A allows an understanding of the contribution of the **g**⟷**e′** pair to dimer stability. E⟷R is 1.33 kcal/mol more stable than A⟷A. Thus, the protein E·R containing eight **g**⟷**e′** pairs over four heptads would be 10.6 kcal/mol more stable than $A \cdot A_{1234}$. One general observation is that most of the **g**⟷**e′** pairs we have examined are more stable than the A⟷A pair. This even extends to some of the homologous interactions that might be expected to be repulsive. For example, K⟷K is 0.34 kcal/mol more stable than A⟷A. Presumably, repulsive effects between the two positively charged lysine amino acids exist, but are compensated for by the hydrophobic packing of the long K side chain across the dimerization interface. Similar results are seen for the R⟷R pair. Only E⟷E has a repulsive interaction and this pair is 0.37 kcal/mol less stable than A⟷A.

The third effect of particular amino acids in the **e** and **g** positions is to regulate dimerization specificity, a direct result of interhelical interactions between the **g** and **e′** amino acids, discussed in detail below.

Interactions between g and e′ amino acids

The use of a thermodynamic cycle analysis allowed us to unravel the interaction energy between the two amino acids in the **g**⟷**e′** pair; this is termed the coupling energy ($\Delta\Delta G_{int}$) (Carter *et al.*, 1984; Horovitz *et al.*, 1990; Serrano *et al.*, 1990). This analysis led to perhaps the most interesting result of this work (Table III). A simple comparison of the E⟷R and E⟷K pairs indicates that E⟷R is 0.35 kcal/mol more stable than E⟷K, the same trend is seen for intrahelical E⟷R and E⟷K pairs (Merutka and Stellwagen, 1991). An examination of the stabilizing contribution of K and R alone (A⟷K and A⟷R) indicates that K is 0.65 kcal/mol more stabilizing than R. The calculation of a coupling energy for each **g**⟷**e′** pair indicates that E⟷R has a $\Delta\Delta G_{int}$ of 1.14 kcal/mol, while E⟷K has a $\Delta\Delta G_{int}$ of only 0.14 kcal/mol. The same general trend is seen when comparing the coupling energies of E and Q with K and R. In each case, R-containing pairs have a stronger $\Delta\Delta G_{int}$ than K-containing pairs. The positive coupling energy of the Q⟷K pair may represent a steric clash between the two amino acids as they hydrophobically pack over the **a** and **d** positions.

Table IV. Energetic difference between E⟷X and Q⟷X pairs (kcal/mol)

↓g/e′→	A	E	Q	R	K
E	−0.14	+0.37	−0.73	−1.33	−0.98
Q	−0.39	−0.46	−1.17	−0.79	−0.83
E−Q	+0.25	+0.83	+0.44	−0.54	−0.15

ΔG values were calculated from CD thermal melts and normalized to A⟷A. The differences between the energetics of E⟷X and Q⟷X pairs have been calculated (E−Q) to emphasize the difference exhibited by E relative to Q.

The very low coupling energy of the E⟷K pair (−0.14 kcal/mol) is consistent with data from Kim's group (O'Shea *et al.*, 1992). These investigators examined the structural specificity required for the preferential heterodimerization of the two bZIP proteins Fos and Jun. They were able to map part of the heterodimerization specificity to the **e** and **g** position of each protein; Fos contains an E⟷E pair, while Jun contains a K⟷K pair and the heterodimer contains both an E⟷K and a K⟷E pair. Lowering the pH to 2 resulted in no change in the dimerization strength of the heterodimer, suggesting the absence of any ion pair attraction in the heterodimer. The absence of any coupling energy between the E⟷K pair and some coupling energy in the calculated K⟷E pair is consistent with the pH experiment.

Structural rational for coupling energy ($\Delta\Delta G_{int}$)

The physical forces that result in the measured coupling energies are unclear. Salt and pH experiments in progress should help to address this question. The type of forces that could exist are van der Waals packing between amino acids, hydrogen bonding between charged or uncharged amino acids (salt independent) or charge−charge interactions (salt dependent) (Scholtz *et al.*, 1993).

Table IV presents a comparison between the stability of E⟷X and Q⟷X pairs (see Figures 7 and 8). Q is structurally similar to a protonated E, which can be created at low pH; both can accept and donate a hydrogen bond. Two structural differences exist between Q and a charged E. Q accepts and donates a hydrogen bond, while E accepts two hydrogen bonds in addition to having possible charge−charge interactions. The difference between the $\Delta\Delta G$ for E⟷X and Q⟷X pairs highlights how these two amino acids interact with the basic amino acids K and R. E⟷K is only −0.15 kcal/mol more stable than Q⟷K while is −0.54 kcal/mol more stable than Q⟷R. E displays a greater range of interaction energies than Q primarily because E⟷E is a very destabilizing interaction. The small energetic difference between E⟷K and Q⟷K (−0.15 kcal/mol) suggests that the possible charge−charge attraction between E and K is not a major contributor to the stability of the pair. The near absence of any coupling energy between E and K ($\Delta\Delta G_{int}$ = −0.14 kcal/mol) independently confirms the absence of any charge−charge interactions. The

large energetic difference between E⟷R and Q⟷R (−0.54 kcal/mol) may reflect the charge−charge contribution to the stability of the E⟷R pair and/or the formation of a second hydrogen bond between the guanidinium group of R and E that is not available with Q. The coupling energy ($\Delta\Delta G_{int}$) between E and R of −1.14 kcal/mol is consistent with a charge interaction and two possible hydrogen bonds between E and R. Electrostatic interactions have been observed in a variety of proteins (Horovitz *et al.*, 1990; Dao-pin *et al.*, 1991; Schmidt-Dor *et al.*, 1991; Robinson and Sligar, 1993). The magnitude of the interactions observed by other investigators is similar to the results presented here. Although individual interaction energies are small, they are important to leucine zipper stability and dimerization specificity because of the large number of such interactions that are possible along the dimer interface.

Heterologous interactions are critical for dimerization specificity

The fact that the strongest **g**⟷**e′** pair (E⟷R) consists of different amino acids allows the design of proteins that preferentially homo or heterodimerize (Figure 12). The difference between the best (E⟷R) and the worst (E⟷E) **g**⟷**e′** pair is 1.7 kcal/mol. Changing a single R to E in each monomer would create a dimer with two new destabilizing interactions, one on each side of the leucine zipper, resulting in a dimer that is 3.4 kcal/mol less stable. This corresponds to a dimerization constant that is 240 times weaker. The energetic contribution of an E⟷R pair to leucine zipper stabilization (−2.66 kcal/mol/heptad) is similar to the contribution of leucine relative to alanine in the **a** (−3.3 kcal/mol) or **d** (−2.0 kcal/mol) position (Zhou *et al.*, 1992). Thus, the **g**⟷**e′** pair can contribute over one-third of the total stabilization of the leucine zipper. Additional experiments with heterologous pairs in the interior of the leucine zipper would be valuable to ascertain if heterologous interactions between **d**⟷**d′** or **a**⟷**a′** could help mediate dimerization specificity. It is expected that further experiments, examining more complex heptads, will provide further details on the structural independence of the **g**⟷**e′** pair.

The large number of leucine zipper proteins in mammalian systems suggests that a judicious combination of attractive and repulsive interactions may be needed to design specific dimerization partners. Since the specificity of dimerization is distributed throughout the length of the leucine zipper, the potential for modulation of dimerization partners is great. Our design of leucine zipper partners that preferentially heterodimerize can be a useful biological tool to bring together different cellular proteins at specific locations in the cell.

Materials and methods

Protein

The sequence of the 96 amino acid host protein is ASMTGGQQMGRDP-LEE-KVFVPDEQKD EKYWTRRKKN NVAAKRSRDA RRLKENQITI RAAFLEKENT ALRTEVAELR KEVGRCKNIV SKYETRYGPL. The 'leucine' positions are in bold type. The first 13 amino acids are from ϕ10 (Studier and Moffatt, 1986), the next three amino acids are a cloning linker and the remaining 80 amino acids are the C-terminus of VBP (Iyer *et al.*, 1991), the chicken equivalent of the mammalian DBP gene (Mueller *et al.*, 1990). These 80 amino acids contain the entire bZIP region of the protein and are able to bind to DNA as a dimer in a sequence-specific manner (Vinson *et al.*, 1993). VBP contains a single cysteine in the **d** position near the C-terminus of the leucine zipper region. This cysteine can be oxidized to form more stable dimers than the reduced protein. Oxidized and reduced proteins display identical helicity at low temperatures. A disulfide bond between cysteines in the **d** position has previously been shown not to disrupt the helix-forming capacity of coiled coils (Zhou *et al.*, 1993). The covalently linked samples bind DNA with similar binding constants to the reduced samples, suggesting that they have similar conformations (data not shown). We have generated two proteins ($E \cdot K_{1234}$ C-S and E·R C-S) where the cysteine has been replaced with serine and found that samples containing a reduced cysteine behave similarly to the serine-containing proteins.

Protein expression and purification

Proteins were synthesized in *E.coli* using the phage T7 expression system (Studier and Moffatt, 1986). Bacterial cultures (400 ml) at an OD of 0.6 at 600 nm were induced with 1 mM IPTG (isopropyl-β-D-thiogalactopyranoside) for 2 h. Cells were recovered by centrifugation, resuspended in 6 ml of lysis buffer [50 mM Tris−HCl (pH 8.0), 1 mM EDTA, 1 mM benzamidine, 1 mM dithiothreitol (DTT) and 0.2 mM phenylmethylsulfonyl fluoride (PMSF)], frozen, thawed and gently brought to 1 M KCl by the addition of 2 ml of 4 M KCl. The samples containing clusters of basic amino acids were gently brought to 2 M KCl before the initial centrifugation. The samples were centrifuged at 25 000 r.p.m. in a Beckman T42 rotor and the supernatant was isolated. The isolated supernatant was then heated to 65°C for 10 min, centrifuged and the supernatant again isolated. The proteins were dialyzed to 20 mM Tris−HCl (pH 8.0), 100 mM KCl, 1 mM EDTA and 1 mM DTT, and loaded onto a heparin agarose column. The column was washed with lysis buffer containing 100 mM KCl, followed by a 300 mM KCl wash, and eluted with buffer containing 1 M KCl. The samples were then dialyzed to 12.5 mM potassium phosphate (pH 7.4), 150 mM KCl, 1 mM EDTA, with or without 1 mM DTT for 48 h with a change of buffer after 24 h. The purity of the proteins was assayed by SDS−PAGE (Laemmli, 1970). The different size proteins used in the gel-shift experiment (Figure 11) were described previously (Vinson *et al.*, 1993).

Construction of mutant proteins

Amino acid substitution mutants were introduced into DBP by the four-primer polymerase chain reaction (PCR) mutagenesis method (Ho *et al.*, 1989). DNA sequencing was performed on double-stranded templates using the Sanger dideoxynucleotide method (Sanger *et al.*, 1977).

Equilibrium sedimentation

Equilibrium sedimentation measurements were performed using a Beckman XL-A Optima Analytical Ultracentrifuge equipped with absorbance optics and a Beckman An-60Ti rotor. Samples were loaded at three concentrations, 10, 20 and 40 μM (0.1, 0.2 and 0.4 OD at 280 nm), into a six-hole centerpiece and spun at 25 000 r.p.m. for 24 h. Twenty data sets for three concentrations were averaged and jointly fitted for a singular mol. wt. Some calculations assumed a monomer−dimer equilibrium. Compositional partial specific volumes for the proteins were calculated according to Zamyatnin (1984). All scans were done at 25°C, except $A \cdot R_{34}$ and $A \cdot K_{34}$ which were done at 10°C.

Circular dichroism studies

CD studies were performed using a Jasco J-710 spectropolarimeter with a 5 mm rectangular CD cell. Temperature scans were performed by scanning continuously from 4 to 80°C at a scan rate of 1°C/min. Data were collected using the time scan mode of the Jasco-710 software. The ellipticity at 222 nm (θ_{222}) was recorded every 1 min with a response time of 5 s and a bandwidth of 1 nm. The temperature in the cell was controlled using a water-jacketed cell holder connected to a Haake F3 circulating water bath equipped with a Haake PG 20 temperature programmer. Temperature was monitored using a Micro-therm 1006 thermometer and an S/N117.c temperature probe in physical contact with the protein solution.

All samples were in 12.5 mM potassium phosphate (pH 7.4), 150 mM KCl, 1 mM EDTA; if there was a cysteine in the protein, 1 mM DTT was added to the sample just before thermal melting and the sample was heated to 65°C for 5 min. All protein concentrations were determined by absorbance at 280 nm in 6 M guanidine hydrochloride using a Hewlett Packard 8425A spectrophotometer assuming the known absorbance for the one tryptophan and four tyrosines in the molecule (Cantor and Schimmel, 1980).

The ellipticity (θ_{222}) of the samples at 2°C, whether cross-linked or not, is 23 700 °·cm²/dmol which suggests that the proteins are ~62% helical (Woody and Tinoco, 1967; Gans *et al.*, 1991). The calculated θ_{222} for a 96 amino acid α-helical protein is ~38 000 °·cm²/dmol. The leucine zipper, assumed to extend from the first **d** position (in this case it is an

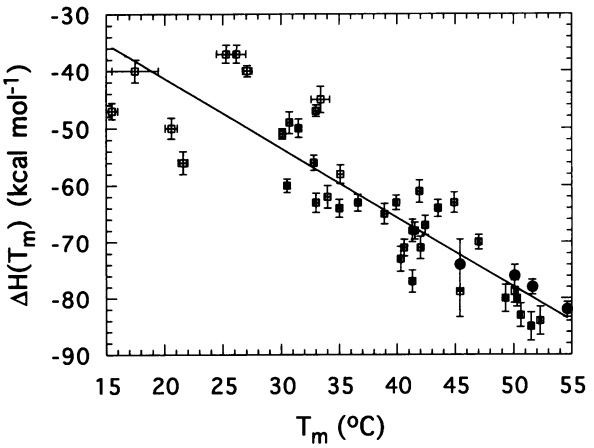

Fig. 14. The van't Hoff enthalpy per mole of dimer at the melting temperature [$\Delta H(T_m)$] is plotted versus the melting temperature (T_m) for four concentrations for EK_4 (●) and various mutant proteins (□). The error from the fitting procedure is shown for both parameters. There is a clear trend for those samples with higher T_m to show a larger $\Delta H(T_m)$. The assumption is that the main contribution to the temperature dependence of $\Delta H(T_m)$ for the various mutant proteins is Δc_p. The slope of the line through all the points was taken as the value of Δc_p (-1.16 ± 0.1 kcal/mol/°) and used to calculate ΔG_o at 37°C. Outliers from this trend exist; proteins containing a large number of unpaired basic residues, e.g. $R \cdot R_{34}$, $A \cdot R_{34}$, $K \cdot K_{34}$, show a smaller than expected $\Delta H(T_m)$, while those containing a large number of acidic residues, e.g. $E \cdot E_{34}$, $E \cdot A_{34}$, have a greater than expected $\Delta H(T_m)$.

isoleucine) all the way to the C-terminus, comprises 45% of the protein. The remaining 17% of unaccounted helicity is assumed to propagate into the basic region from the leucine zipper (Saudek *et al.*, 1991).

Calculation of thermodynamic parameters

Thermodynamic parameters were determined by curve fitting of the denaturation curves to the following equations using a non-linear least-squares fitting program (KaleidaGraph, Synergy Software). Ellipticity was normalized to fraction monomer using the equation:

$$\theta = (\theta_M - \theta_D)P_M + \theta_D \quad (1)$$

where θ_M and θ_D represent the ellipticity values for the fully unfolded monomer and fully folded dimer species at each temperature. θ_M was found to be constant at the temperatures higher than the melting region for all the proteins studied. θ_D was approximated by a linear function of temperature $\theta_D = \theta_D(0) + \alpha T$. The fraction monomer ($P_M$) was expressed in terms of the equilibrium constant after solving the equation for a bimolecular reaction $2M \leftrightarrow D$:

$$P_M = [(8KC + 1)^{1/2} - 1]/4KC \quad (2)$$

where K is the equilibrium constant and C is the total protein concentration. K was assumed to be temperature dependent according to the equation

$$K = e^{-\Delta G/RT} \quad (3)$$

This equation was expressed in terms of ΔH_m, the slope of the curve at T_m

$$K = C^{-1}\exp\{\Delta H_m(1/T_m - 1/T)/R + \Delta cp[T_m - T + T\ln(T/T_m)/R]\} \quad (4)$$

where T_m is the melting temperature ($P_M = 1/2$), ΔH_m is van't Hoff enthalpy of dimerization, Δc_p is the heat capacity change and R is the gas constant. Equations (1), (2) and (4) were combined and fitted to the CD data using KaleidaGraph fitting for the five parameters T_m, ΔH_m, α, θ_U and $\theta_F(0)$. We were unable to simultaneously solve for both ΔH_m and Δc_p because of the high degree of interdependence of these two variables. More satisfactory results were obtained by initially assuming Δc_p to be zero and then determining its value as described below. Δc_p could be calculated from the dependence of ΔH_m on T_m observed either by varying the concentration of a particular protein or using similar concentrations of different mutant proteins. Both methods gave similar results for Δc_p (Figure 14). This value of Δc_p has been used in our computations to calculate ΔG_o at the reference temperature $T_o = 37$°C:

$$\Delta G_o = RT_o\ln C - \Delta H_m(T_o/T_m - 1) - \Delta c_p\,[T_m - T_o + T_o\ln(T_o/T_m)] \quad (5)$$

The calculation of the thermodynamic parameters for heterodimers is complicated by the presence of three dimeric species. However, if an equimolar mixture of two proteins has a T_m which is significantly higher than that of either homodimer, it is possible to determine thermodynamic parameters of the heterodimer from the melting curve. In this case, the protein concentration (C) in equation (4) is the concentration of each protein. As a result, the total protein concentration in the mixing experiments was twice that in homodimer experiments.

The choice of the fitting interval from the CD melting curves affects the obtained thermodynamic parameters and results in an error of ΔG_o ranging from 0.1 to 0.4 kcal/mol. Three independent protein preparations of the same sample ($E \cdot K_{1234}$ C-S) have a ΔG_o range of 0.17 kcal/mol.

Calculation of heterodimer formation

When two proteins, capable of homo- and heterodimerization, are present in solution, the following three reactions take place:

$$2M_1 \leftrightarrow D_1, \quad [D_1]/[M_1]^2 = k_1 = e^{-\Delta G1/RT} \quad (6)$$

$$2M_2 \leftrightarrow D_2, \quad [D_2]/[M_2]^2 = k_2 = e^{-\Delta G2/RT} \quad (7)$$

$$M_1 + M_2 \leftrightarrow HD, \quad [HD]/[M_1][M_2] = k_3 = 2e^{-\Delta G^*HD/RT} \quad (8)$$

(Note that in the last equation, ΔG^*_{HD} stands for an 'intrinsic' free energy of heterodimer formation. In this case, the exponential term is multiplied by two because two of four monomer collisions favor heterodimer while only one gives rise to each homodimer.) Because reactions (1)–(3) are linked, the concentration of heterodimer is related to the concentrations of homodimers:

$$[HD] = 2([D_1][D_2])^{1/2}\, e^{-\Delta G\text{specificity}/RT} \quad (9)$$

where $\Delta G_{specificity} = \Delta G^*_{HD} - (\Delta G_1 + \Delta G_2)/2$.

Equation (4) shows that for the preferential formation of heterodimer, $\Delta G_{specificity}$ should be large and negative. If homodimers and heterodimer are equally stable, $\Delta G_{specificity} = 0$, thus $[HD] = 2([D_1][D_2])^{1/2}$. Therefore, the heterodimer concentration can never exceed the sum of concentrations of homodimers, in the case of equal homodimer concentrations we will have the well-known ratio describing indifferent association with the heterodimer being twice as abundant as either homodimer $[D_1]:[HD]:[D_2] = 1:2:1$. The same relationship between heterodimer formation and dimer concentration will be exhibited by molecules which dimerize with different stability, but contribute to the stability of heterodimer independently (the heterodimer has no novel interactions compared to the homodimers) so that $\Delta G^*_{HD} = (\Delta G_1 + \Delta G_2)/2$ and $\Delta G_{specificity} = 0$ (Figure 11). When the heterodimer contains novel interactions when comparing to homodimers, its concentration could be either much greater (if $\Delta G_{specificity}/RT << 0$, see Figure 12) or much less (if $\Delta G_{specificity}/RT >> 0$) than the concentrations of homodimers. Knowing the dimerization free energy for given proteins, we will be able to predict the ratio $[HD]/2([D_1]^*[D_2])^{1/2}$, reflecting the specificity of dimerization.

Acknowledgements

We thank Ernesto Friere, Kelly Thompson and the Biocalorimetry Center for use of the spectropolarimeter (NIH RR-04328), Mark Lewis for help with the XLA, and Mike Fritch and Carl Wu for the mass spectrometer analysis. We thank B.K.Lee and B.Garcia-Moreno for thoughtful discussions throughout this work, and V.Vinson, A.S.H.Goldman and members of the laboratory for comments on the manuscript. We thank J.Eldridge for the oligonucleotide synthesis and Claude Klee for encouragement and support.

References

Agre,P., Johnson,P. and McKnight,S. (1989) *Science*, **246**, 922–925.
Alber,T. (1992) *Curr. Opin. Genet. Dev.*, **2**, 205–210.
Alberti,S., Oehler,S., Wilcken-Bergmann,B.V. and Muller-Hill,B. (1993) *EMBO J.*, **12**, 3227–3236.
Amati,B., Brooks,M., Levy,N., Littlewood,T., Evan,G. and Land,H. (1993) *Cell*, **72**, 233–246.
Baxevanis,A. and Vinson,C. (1993) *Curr. Opin. Genet. Dev.*, **3**, 278–285.
Blaber,M., Zhang,X.-J. and Matthews,B. (1993) *Science*, **260**, 1637–1640.
Cantor,C. and Schimmel,P. (1980) *Biophysical Chemistry*. W.H.Freeman, New York.
Cao,Z., Umek,R. and McKnight,S. (1991) *Genes Dev.*, **5**, 1538–1552.
Carter,P., Winter,G., Wilkinson,A. and Fersht,A. (1984) *Cell*, **38**, 835–840.
Cohen,C. and Parry,D. (1990) *Protein*, **7**, 1–14.
Cooper,T. and Woody,R. (1990) *Biopolymers*, **30**, 657–676.
Crick,F. (1953) *Acta. Crystallogr.*, **6**, 689–697.

Dao-pin,S., Sauer,U., Nicholson,H. and Matthews,B. (1991) *Biochemistry*, **30**, 7142–7153.
Ellenberger,T., Brandl,C., Struhl,K. and Harrison,S. (1992) *Cell*, **71**, 1223–1237.
Fairman,R., Shoemaker,K., York,E., Stewart,J. and Baldwin,R. (1990) *Biophys. Chem.*, **37**, 107–119.
Gans,P., Lyu,P., Manning,M., Woody,R. and Kallenbach,N. (1991) *Biopolymers*, **31**, 1605–1614.
Gentz,R.,III, Rauscher,J.F., Abate,C. and Curran,T. (1989) *Science*, **243**, 1695–1699.
Graddis,T., Myszka,D. and Chaiken,I. (1993) *Biochemistry*, **32**, 12664–12671.
Hai,T. and Curran,T. (1991) *Proc. Natl Acad. Sci. USA*, **88**, 3720–3724.
Hai,T., Liu,F., Coukos,W. and Green,M. (1989) *Genes Dev.*, **3**, 2083–2090.
Harbury,P., Zhang,T., Kim,P. and Abler,T. (1993) *Science*, **262**, 1401–1407.
Ho,S., Hunt,H., Horton,R., Pullen,J. and Pease,L. (1989) *Gene*, **77**, 51–59.
Hodges,R., Sodak,J., Smillie,L. and Jurasek,L. (1972) *Cold Spring Harbor Symp. Quant. Biol.*, **37**, 299–310.
Horovitz,A., Serrano,L., Avron,B., Bycroft,M. and Fersht,A. (1990) *J. Mol. Biol.*, **216**, 1031–1044.
Hu,J., O'Shea,E., Kim,P. and Sauer,R. (1990) *Science*, **250**, 1400–1403.
Hu,J., Newell,N., Tidor,B. and Sauer,R. (1993) *Protein Sci.*, **2**, 1072–1084.
Ivashkiv,L.B., Liou,H.-C., Kara,C.J., Lamph,W.W., Verma,I.M. and Glimcher,L.H. (1990) *Mol. Cell. Biol.*, **10**, 1609–1621.
Iyer,S., Davis,D., Seal,S. and Burch,J. (1991) *Mol. Cell. Biol.*, **11**, 4863–4875.
Konig,P. and Richmond,T. (1993) *J. Mol. Biol.*, **233**, 139–154.
Kouzarides,T. and Ziff,E. (1988) *Nature*, **336**, 646–651.
Kouzarides,T. and Ziff,E. (1989) *Nature*, **340**, 568–571.
Laemmli,U. (1970) *Nature*, **277**, 680–685.
Landschultz,W., Johnson,P. and McKnight,S. (1988) *Science*, **240**, 1759–1764.
Landschultz,W., Johnson,P. and McKnight,S. (1989) *Science*, **243**, 1681–1688.
Loriaux,M., Rehfuss,R., Brennan,R. and Goodman,R. (1993) *Proc. Natl Acad. Sci. USA*, **90**, 9046–9050.
Lovejoy,B., Choe,S., Casio,D., McRorie,D., DeGrado,W. and Eisenberg,D. (1993) *Science*, **259**, 1228–1293.
Lye,P., Liff,M., Marky,L. and Kallenbach,N. (1990) *Science*, **250**, 669–673.
Marqusee,S. and Baldwin,R. (1987) *Proc. Natl Acad. Sci. USA*, **84**, 8898–8902.
Merutka,G. and Stellwagen,E. (1991) *Biochemistry*, **30**, 1591–1594.
Mueller,C., Maire,P. and Schibler,U. (1990) *Cell*, **61**, 279–291.
Murre,C., McCaw,P. and Baltimore,D. (1989) *Cell*, **56**, 777–783.
Nicklin,M. and Casari,G. (1991) *Oncogene*, **6**, 173–179.
Nilges,M. and Brunger,A. (1991) *Protein Eng.*, **4**, 649–659.
O'Neil,K. and DeGrado,W. (1990) *Science*, **250**, 646–651.
O'Shea,E., Rutkowski,R., Stafford,W. and Kim,P. (1989) *Science*, **254**, 539–544.
O'Shea,E., Klemm,J., Kim,P. and Abler,T. (1991) *Science*, **254**, 539–544.
O'Shea,E., Rutkowski,R. and Kim,P. (1992) *Cell*, **68**, 699–708.
O'Shea,E., Lumb,K. and Kim,P. (1993) *Curr. Biol.*, **3**, 658–667.
Padmanabhan,S., Marqusee,S., Ridgeway,T., Laue,T. and Baldwin,R. (1990) *Nature*, **344**, 268.
Pu,W. and Struhl,K. (1993) *Nucleic Acids Research*, **21**, 4348–4355.
Robinson,C. and Sligar,S. (1993) *Protein Sci.*, **2**, 826–837.
Roman,C., Platero,J., Shuman,J. and Calame,K. (1990) *Genes Dev.*, **4**, 1404–1415.
Sanger,F., Nicklen,S. and Coulson,A. (1977) *Proc. Natl Acad. Sci. USA*, **74**, 5463–5467.
Saudek,V., Pastore,A., Castiglione-Morelli,M., Frank,R., Gausepohl,H. and Gibson,T. (1991) *Protein Eng.*, **4**, 519.
Schindler,U., Menkens,A.E., Beckman,H., Ecker,J.R. and Cashmore,A.R. (1992) *EMBO J.*, **11**, 1261–1273.
Schmidt-Dor,T., Oertel-Buchheit,P., Pernelle,C., Bracco,L., Schnarr,M. and Granger-Scharr,M. (1991) *Biochemistry*, **30**, 9657–9664.
Scholtz,J., Qian,H., Robbins,V. and Baldwin,R. (1993) *Biochemistry*, **32**, 9668–9676.
Schuermann,M., Hunter,J., Hennig,G. and Muller,R. (1991) *Nucleic Acids Res.*, **19**, 739–746.
Serrano,L., Horovitz,A., Avron,B., Bycroft,M. and Fersht,A. (1990) *Biochemistry*, **29**, 9343–9352.
Studier,F. and Moffatt,B. (1986) *J. Mol. Biol.*, **189**, 113–130.
Thompson,K., Vinson,C. and Freire,E. (1993) *Biochemistry*, **32**, 5491–5496.
Turner,R. and Tjian,R. (1989) *Science*, **243**, 1689–1694.
Vinson,C., Sigler,P. and McKnight,S. (1989) *Science*, **246**, 911–916.
Vinson,C., Hai,T. and Boyd,S. (1993) *Genes Dev.*, **7**, 1047–1058.
Williams,S., Cantwell,C. and Johnson,P. (1991) *Genes Dev.*, **5**, 1553–1567.
Woody,R. and Tinoco,I. (1967) *J. Chem. Phys.*, **46**, 4927–4945.
Zamyatnin,A. (1984) *Annu. Rev. Biophys. Bioeng.*, **13**, 145–165.
Zhou,N., Kay,C. and Hodges,R. (1992) *Biochemistry*, **31**, 5739–5746.
Zhou,N., Kay,C. and Hodges,R. (1993) *Biochemistry*, **32**, 3178–3187.

Received on February 11, 1994; revised on April 11, 1994